

Heats of adsorption of Pb on pristine and electron-irradiated poly(methyl methacrylate) by microcalorimetry

S.F. Diaz¹, J.F. Zhu¹, J.J.W. Harris, P. Goetsch, L.R. Merte, Charles T. Campbell*

Department of Chemistry, University of Washington, Box 351700, Seattle, WA 98195-1700, USA

Received 6 May 2005; accepted for publication 15 September 2005

Available online 5 October 2005

Abstract

The heat of adsorption and sticking probability were measured for Pb gas atoms adsorbing onto clean poly(methyl methacrylate) (PMMA) and electron-irradiated PMMA. The Pb atoms interact very weakly with the outgassed pristine PMMA surface, with a sticking probability of 0.02 ± 0.02 . They deposit a heat into the PMMA of 12.7 ± 0.7 kJ/mol of dosed Pb, independent of Pb exposure up to 10 ML. This is slightly less than would be expected even if no Pb atoms stuck to the PMMA, but if they completely thermally accommodated to the substrate temperature during their collision with the surface. This proves that thermal accommodation is incomplete, highlighting the weakness of the Pb–PMMA interaction. Damaging the PMMA surface with electrons causes an increase in reactivity with Pb, as shown by increases in the initial heat of adsorption up to 134.0 ± 0.7 kJ/mol and the initial sticking probability up to 0.51 ± 0.01 . These both increase with increasing coverage toward the values expected for Pb adsorption onto a bulk Pb surface with coverage dependences suggesting that metal islands nucleate at electron-induced defects, and grow into large 3D islands of low number density. This is the first calorimetric measurement of any metal adsorption energy onto any polymer surface wherein the sticking probability of the metal also was measured. The PMMA film was spin coated directly onto the heat detector, a pyroelectric polymer foil (polyvinylidene fluoride—PVDF) precoated on both sides with thin metal electrodes. It provides a detector sensitivity of ~ 450 V/J with a pulse-to-pulse standard deviation of 1.2 kJ/mol and absolute accuracy within 2%.

© 2005 Elsevier B.V. All rights reserved.

Keywords: Polymer surface; Heat of adsorption; Metal adsorption; Adsorption calorimetry; Pb; Poly(methyl methacrylate); Electron damage; Sticking probability

* Corresponding author. Tel.: +1 206 616 6085; fax: +1 206 616 6250.

E-mail addresses: campbell@chem.washington.edu, surfacesci@chem.washington.edu (C.T. Campbell).

¹ These two authors contributed equally to this manuscript, and should share first authorship.

1. Introduction

Metal/polymer interfaces are important in wide-ranging applications including a variety of coatings [1] as well as organic microelectronic and optoelectronic devices such as organic light emitting diodes (OLED), organic field effect transistors (OFET), organic photovoltaics (OPV), and organic electro-optic modulators [2,3]. Though important from both technological and fundamental viewpoints, the strength of chemical bonding at the metal/polymer interface has rarely been studied. Not only is strength required for a stable interface, but its bond energetics may correlate with important electric properties of the interface such as the interface band offset [4].

Several reviews on thin film morphology and diffusion characteristics of vapor deposited metals on, and into, polymer substrates as studied by surface sensitive techniques (most notably XPS, AFM and TEM) are available in the literature [5–8]. Generally speaking, metal reactivity on polymers can be broken into two groups: strongly reactive metals such as Cr, Ni, or Al which have a tendency to significantly interact with the polymer chains found at the surface, often wetting the surface, and weakly reactive metals such as Cu, Ag, or Au which exhibit a great deal more mobility on, and into, the polymer [6,9]. The polymer functionality should also play a role in the strength of metal/polymer reactivity, since polymers with functional groups containing nitrogen or oxygen species show a preference for the formation of metal–nitrogen–carbon or metal–oxygen–carbon complexes over the less selective binding of metals onto polymers containing only hydrocarbons [9–11]. Vapor phase metal atoms can alter the polymer surface upon adsorption, forming amorphous carbon and metal nitride or metal oxide moieties at the interface [9]. In practice, the reactivity of nearly all polymer surfaces toward metals is improved by exposure of the polymer surface to electron beams, ion beams or UV radiation [12].

Poly(methyl methacrylate) (PMMA) exhibits a number of desirable properties including moderate cost, mechanical and thermal stability, and impressive optical properties which makes it one of the most widely used polymers in manufacturing

[13,14]. The ease and control in which PMMA can be spin coated onto surfaces has led to its use as a resist layer in integrated circuit (IC) manufacturing [15], making an understanding of metal/PMMA bonding at the interface critical for proper IC production. Vapor depositing metals onto PMMA has also risen in prominence in the construction of micro-optics, particularly lenses and mirrors [14]. Fig. 1 shows the structural model of PMMA. The ester of the pendant group is thought to be the center of metal reactivity in this polymer [11,16], though some have claimed that it is not the availability of oxygen that determines reactivity but the surface energy of the polymer [17].

Electron or ion beam damage has been found to increase the reactivity of PMMA surfaces towards metals, and has been used to improve metal/PMMA adhesion [18]. Ion and electron beam damage have been shown to create bond scission in the PMMA polymer chains, polymer cross-linking, dehydrogenation, deoxygenation and creation of surface radicals [15,18–20]. Ion beam damage has also been shown to increase the glass transition temperature (T_g) in polystyrene [21], the predominant factor determining the degree of metal diffusion into the bulk of the polymer [6]. Despite increased Cu reactivity on ion beam damaged PMMA, low energy ion spectroscopy (LEIS) shows that the ester groups are reoriented toward the bulk on the pristine surface, yet the O/C LEIS ratio goes down with bombardment [18], indicating that the ester group may not be the main reaction center for the metals after ion damage. The most likely defect sites leading to metal nucleation are surface radicals and the unsaturated bonds they create within a polymer chain [18].

Metal adsorption calorimetry, which measures the energy released as the metal/polymer bonds

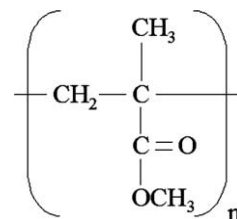


Fig. 1. Repeat unit of poly(methyl methacrylate) (PMMA).

form upon metal adsorption, provides direct information regarding the strength of the metal/polymer chemical bonding. Bond energies are of fundamental importance, and directly related to the adhesion energy of adsorbed metal films on polymers.

The first calorimeter designed to measure the heat evolved during metal vapor adsorption onto polymers was developed by Stuckless et al. [22–24]. Drawing inspiration from single crystal adsorption calorimeters developed by King [25] and Campbell [26], Stuckless directly spin-coated polymers onto LiTaO₃ [23], creating a self-contained pyroelectric detector unit [23,24] capable of achieving pulse-to-pulse standard deviations as small as 4 kJ/mol [23,24]. Their first studies (Ca, Cu, and Cr adsorption on pyromellitic dianhydride-oxydianiline (PMDA–ODA) [23]) showed that the nature of the metal plays a strong role in the strength of binding at the metal/polymer interface: Ca forms a bond to the PMDA–ODA surface that is ~500 kJ/mol stronger than to itself, while Cr exhibits a surprisingly weak metal/polymer bond (125 kJ/mol), though proper analysis is hindered by their lack of sticking probability data [23]. They also showed that Cu binds so weakly to PMDA–ODA that its heat of adsorption is dominated by Cu–Cu binding in Cu clusters that immediately nucleate on the surface [23]. Stuckless and co-workers also used their calorimeter to probe the role of different organic functional groups at metal/polymer interfaces, particularly the influence of the vinylene group found in (poly[2-methoxy, 5-(2'-ethyl-hexyloxy)-*p*-phenylene-vinylene]) (MEH-PPV) and its lack in (MEH-PP), finding that Ca reacts strongly with the MEH-PPV while being nearly unreactive with MEH-PP [24].

This paper presents the calorimetrically-measured heat of adsorption and sticking probability of Pb adsorption on a clean (“pristine”) and electron pre-irradiated 1 μm PMMA films spin-coated onto pyroelectric PVDF circlets. To our knowledge, this is the first calorimetric measurement of the energetics of metal adsorption on PMMA, and the first calorimetric measurement of any metal onto any organic or polymer film surface wherein the sticking probability of the metal atoms striking the surface was measured also.

The sticking probability must be known in order to determine the adsorption energy per adsorbed metal atom. We demonstrate here a pulse-to-pulse standard deviations in the measured heats of 0.7 kJ/mol and absolute accuracy within 3 kJ/mol, which represent marked improvements over any previous measurements of metal adsorption heats on polymers.

2. Experimental details

The calorimeter’s heat detector is a 1.3 cm diameter circular sheet of a pyroelectric polymer (β -polyvinylidene fluoride or PVDF), precoated with 20–60 nm of NiAl on both faces for electrical contacts. This poled PVDF ribbon generates a face-to-face voltage in response to a heat input generated by metal vapor adsorption. It was cut out of a large sheet of metal-precoated PVDF (available from Measurement Specialties, Inc.) with ceramic scissors to avoid face-to-face shorts. The polymer of interest (PMMA here) was spin-coated directly on the front face of this PVDF sheet, to ensure maximum thermal contact. This polymer-coated pyroelectric detector sheet was then clamped onto a specially designed sample platen so that it could be moved around with sample forks and so that its voltage could be accessed inside an ultrahigh vacuum calorimetry/surface analysis chamber. A complete description of the sample/calorimeter platen design and the sample preparation chamber used for these experiments is provided in the accompanying [Appendix A](#).

The calorimetric method used here is an adaptation of our metal adsorption calorimetry procedure described previously [26–29]. A new sample/calorimeter platen is introduced for each fresh polymer film. This platen is mounted on the platen holder, which itself is mounted on a large Cu thermal reservoir mounted inside an ultrahigh vacuum (UHV) surface analysis chamber, described in [29]. A pulse of gaseous metal atoms from a chopped and collimated (4 mm diameter) atomic beam impinges on the surface of the spin-coated polymer, and partially adsorbs. The energy from gas adsorption generates a transient temperature rise in the sample, which is transferred by thermal

diffusion to the pyroelectric PVDF heat-detecting element. The resulting peak-to-peak voltage response (“signal”) is calibrated using the voltage response to pulses of known energy from a He–Ne laser, as in [26–29]. A sensitivity of $\sim 450 \text{ V/J}_{\text{abs}}$ (volts per joule of heat absorbed by the PMMA) was commonly found.

The UHV chamber (“analysis chamber”) is equipped with a hemispherical electron energy analyzer (Leybold-Heraeus EA 11/100) for Auger electron spectroscopy (AES), a quadrupole mass spectrometer (QMS) (UTI), an ion gun, and a quartz crystal microbalance. The analysis chamber and the pulsed metal atomic beam used in this study were the same as those described in [26]. The UHV chamber has a base pressure of $\sim 2 \times 10^{-10}$ mbar. Adjacent to the analysis chamber is a small sample preparation chamber where samples could be stored, outgassed, and shuttled into the analysis chamber (see Appendix A). The sample preparation chamber has a base pressure of $\sim 8 \times 10^{-9}$ mbar.

Poly(methyl methacrylate) (PMMA) (MW = $\sim 15,000$ amu, Sp^2 Scientific Polymer Products, Inc.) films were deposited directly on the metalized PVDF circlets by ex situ spin-coating of a 5.2% (w/v) PMMA in a chloroform (99.25% purity) solution applied at 2000 rpm for 30 s. Ellipsometry measurements of PMMA films cast on a SiO_2 substrate in a similar manner estimated film thicknesses of $\sim 1 \mu\text{m}$ [30]. The reflectivity of each sample for the He–Ne laser was then measured using an integrating sphere and found to be ~ 0.87 . Atomic force microscopy measurements show that the thin PMMA film is flat and homogeneous.

A collection of PMMA samples, spin coated on PVDF calorimeter detectors and installed in their platens, were mounted on the sample platen carriage in the sample holding chamber and evacuated to below 3×10^{-8} mbar. Here, they were heated to $\sim 335 \text{ K}$ for 24 h before measurements and to 350 K for 30 min just before use. Individual samples were then transferred into the analysis chamber for study. An AES spectra of a representative sample did not show a Cl peak, indicating that the 350 K curing is sufficient to completely evaporate the spin coating solvent. Samples pre-

pared in this manner are referred to as “pristine” PMMA in this paper.

In some cases, the pristine PMMA surface was exposed to an electron source to create an “electron-irradiated” PMMA film. The sample platen, which supports the pristine PMMA film, was held at a positive sample bias of 155 V relative to the hot filament electron source and the PMMA was exposed to a measured electron flux of $6 \mu\text{A}/\text{cm}^2$ for 10 min (i.e., $4.7 \times 10^{16} \text{ e}^-/\text{cm}^2$) using 155 eV electrons.

The metal atom beam is produced from 99.9999% purity Pb pellets (Alfa Aesar) which is evaporated from an effusive vapor source. The metal atom beam is collimated through a series of orifices such that a deposition spot of $\sim 4 \text{ mm}$ in diameter is projected onto the PMMA sample. The beam is chopped into 0.1 s long pulses which deliver $\sim 0.018 \text{ ML}$ of Pb every 2 s (1 ML is defined as $9.425 \times 10^{14} \text{ atoms}/\text{cm}^2$, which is the Pb(111) atomic density). The operating temperature of the oven to maintain this flux is $\sim 1120 \text{ K}$, which generates some thermal optical radiation that impinges on the sample and also is detected by the calorimeter ($\sim 0.3 \mu\text{J}/\text{pulse}$, or $\sim 77.0 \pm 0.3 \text{ kJ}$ of absorbed radiation per mole of dosed Pb). This thermal radiation is measured by blocking the metal beam with a BaF_2 window, which stops the metal atoms from impinging on the PMMA surface, but allows a known fraction of the radiation ($\sim 95\%$, measured before and after each experiment with a laser of known power) to pass and be detected by the calorimeter. This radiation contribution is subtracted from the total measured signal. To convert these measured internal energy changes into the standard enthalpy change at the surface temperature (300 K), the excess translational energy of the metal gas atoms at the oven temperature above that for a 300 K Maxwell–Boltzmann distribution ($\sim 0.05 \mu\text{J}/\text{pulse}$) is subtracted, and a small pressure–volume work term (RT) is added, as described elsewhere [26]. As the metal coverage increases, one would expect that the heats would eventually reach the enthalpy of sublimation of the adsorbing metal at 300 K.

The measured heats can be expressed as molar heats of reaction (heat released per mole adsorbed), provided that the amount of Pb adsorbed with

each pulse is known. Towards this end, the incident metal beam flux is measured using a quartz crystal microbalance. The fraction of an incident metal pulse that adsorbs onto the PMMA surface (i.e., the sticking probability) is measured by a modified King–Wells method [31], which uses a line-of-sight quadrupole mass spectrometer to measure the percentage of metal atoms that strike the surface, but that do not adsorb. The QMS is mounted at 35° from the sample normal (the so-called “magic angle”) to minimize the angular dependence of the signal [26,32]. The reflected signal is calibrated to a zero sticking reference, the signal from a Ta foil heated to a temperature (>900 K) where all incident Pb atoms desorb, corrected for the average velocity of the atoms assuming they have thermally accommodated to the Ta foil [26].

We estimate the accuracy of the absolute calibration of this calorimeter to be within $\sim 2\%$ for metals with sticking probabilities above 90%. This is estimated based on the cumulative errors in absolute calibration of the metal flux, the laser power and the reflectivity of the sample. For metals with low sticking probabilities, this error increases in a complex way as described below.

3. Results

3.1. Sticking probability measurements

3.1.1. Pb on pristine PMMA

A representative measurement of the sticking probability at 300 K for Pb onto the pristine PMMA surface as a function of coverage is shown in Fig. 2. The initial sticking probability starts at 0.02 ± 0.02 and remains near that value for all measured coverages, and any observed fluctuations are likely due to shifting metal flux during the course of the measurement. (Large percentage errors in sticking probability always result when the sticking probability is so low, since it involves subtracting two very similar numbers.)

Comparison of the line shape of the quadrupole mass spectrometer response from scattered metal beam pulses to the instrument response function (not shown) indicate that the residence time of

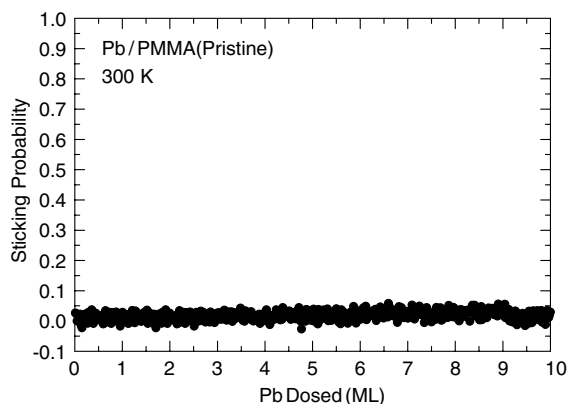


Fig. 2. The sticking probability of Pb onto an undamaged, spin-coated pristine PMMA surface at 300 K as a function of the amount of Pb dosed onto the surface. Each data point is due to a pulse of approximately 0.018 ML of Pb.

any transiently adsorbed metal species on the surface (as observed by the decay in their signal at the end of a pulse) was less than ~ 5 ms, the response time of the beam chopper cut-off, for all observed coverages [33]. Assuming a desorption prefactor of 10^{15} s^{-1} , this places a limit of <73 kJ/mol on the adsorption energy of the Pb atoms, if they were transiently adsorbed, rather than simply inelastically scattered.

As will be discussed below, the reflected Pb atoms do not completely thermally accommodate to the PMMA surface, as they are observed to have a kinetic energy slightly greater than that for 300 K. Thus, the values of sticking probability shown in Fig. 2 are probably too large, since the mass spectrometer signal of the non-sticking fraction was corrected for its thermal velocity [26], assumed here to be the sample temperature.

3.1.2. Pb on electron beam irradiated PMMA

The measured sticking probability at 300 K for Pb onto the electron-modified PMMA surface is shown in Fig. 3 as a function of the amount of dosed Pb. This curve is the average of three sticking measurements. The solid curve is an analytical fit to the data, and was used to convert the amount of Pb dosed onto the electron irradiated surface into adsorbed Pb coverage. The fit was made to an equation of the form

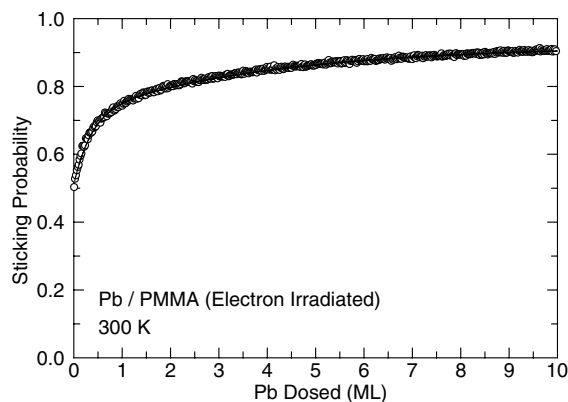


Fig. 3. The sticking probability of Pb onto an electron-irradiated, spin-coated PMMA surface at 300 K as a function of the amount of Pb dosed onto the surface. Each data point is due to a pulse of approximately 0.018 ML of Pb. The data is the average of three experimental runs. The solid curve is the fit line used to determine the coverage. The electron exposure was $6 \mu\text{A}/\text{cm}^2$ ($4.7 \times 10^{16} \text{e}^-/\text{cm}^2$) of 155 eV electrons for 10 min.

$$y = y_0 + a(1 - e^{-bx}) + c(1 - e^{-dx}), \quad (1)$$

where y is the sticking probability, x is the cumulative amount of Pb dosed in ML, and the best-fit parameters were: $y_0 = 0.51$, $a = 0.206$, $b = 2.79$, $c = 0.20$, and $d = 0.287$.

As is observed, the initial sticking probability is 0.51 ± 0.01 and rises with coverage to ~ 0.92 at 9 ML. The trend of increasing sticking probability with coverage is similar to systems where adsorbed metals form clusters at nucleation centers followed by 3D cluster growth slowly covering the surface, such as occurs for metal deposition on many oxide surfaces [34–36].

These nucleation centers can be formed on the surface with minimal electron beam exposure. A PMMA surface which had been exposed to only $6 \mu\text{A}/\text{cm}^2$ of 155 eV electrons for 15 s (not shown) gave an initial sticking probability of 0.025 and linearly increased to 0.20 after ~ 8 ML of Pb dosed.

3.2. Adsorption calorimetry measurements

3.2.1. Pb on pristine PMMA

The calorimetrically measured heats of collision for Pb atoms striking the pristine, spin-coated PMMA surface at 300 K are shown in Fig. 4 as a function of the amount of dosed Pb. This curve

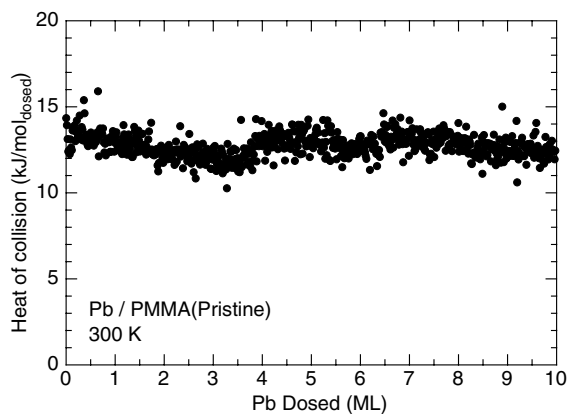


Fig. 4. The measured heat transferred to the polymer for collisions of the Pb atoms from the atomic beam with undamaged, spin-coated PMMA at 300 K, plotted as a function of the amount of Pb that was dosed to the surface (i.e., the Pb exposure, uncorrected for the low sticking probability). Each data point is due to a pulse of approximately 0.018 ML of Pb. No correction has been made for the difference in kinetic energy of the incoming Pb gas and their energy as they thermally accommodate to the surface temperature (see text). That is, this shows the uncorrected heat input to the sample due to each gas pulse, divided by the number of moles that struck the sample in that pulse. This is an average of four experimental runs.

is the average of four individual calorimetry runs. Note that in Fig. 4 we have not made the usual correction due to hot Pb atoms thermally accommodating to the sample surface nor have we subtracted the RT term which converts the measured energy into an enthalpy. For this reason we refer to the heats here not as heats of adsorption, but instead as “heats of collision”, that is, the net heat imparted to the sample due to collisions of the gaseous metal atom beam, per mole of metal gas colliding with the surface.

The initial heat is $13.3 \text{ kJ}/\text{mol}_{\text{dosed}}$, and remains near this value (averaging $12.7 \text{ kJ}/\text{mol}_{\text{dosed}}$) for all measured coverages. The standard deviation of the measured data points is $\pm 0.7 \text{ kJ}/\text{mol}_{\text{dosed}}$. Although $13 \text{ kJ}/\text{mol}_{\text{dosed}}$ is small compared to the thermal radiation originating from the oven ($77 \text{ kJ}/\text{mol}$), the error associated with the radiation measurement is much smaller ($\sim 0.3 \text{ kJ}/\text{mol}$). The very low heats observed here highlight the inertness of this surface toward Pb atoms. Due to the very low sticking probability seen here (Fig. 2), there is a large relative error in the sticking probability at

a given metal dose, which would propagate into an even larger error in coverage versus dosed amount. This also leads to a large error in estimating the percentage of thermal energy lost by “hot” metal gas atoms that do not stick to the substrate (see below).

3.2.2. Pb on electron-irradiated PMMA

Shown in Fig. 5 are the heats of adsorption of Pb onto the electron beam modified PMMA surface as a function of Pb coverage, averaged over three experimental runs. The electron exposure was the same as Fig. 3. The initial heat of adsorption starts at 134.0 kJ/mol with the first 0.018 ML of Pb deposited, much lower than the heat of sublimation of Pb. Note that in Fig. 5 the thermal energies of hot adsorbates and the RT correction converting heats into enthalpies have been applied here, as addressed in the experimental section, and that the coverage axis is now in terms of Pb ML adsorbed onto the PMMA. The heat of adsorption

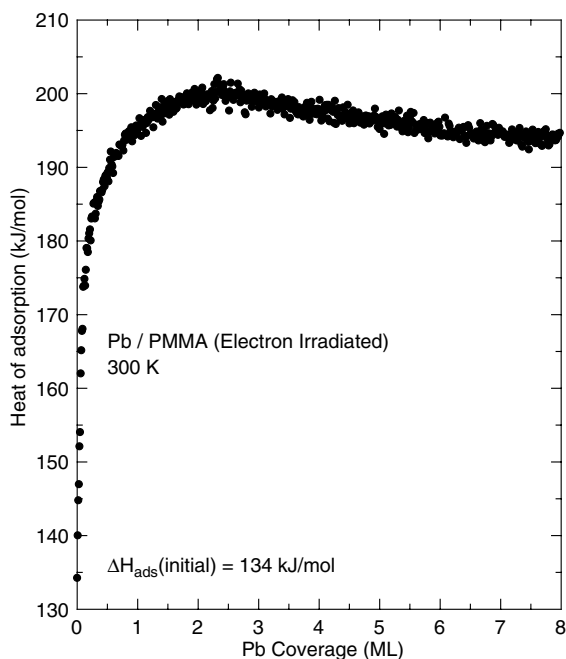


Fig. 5. The measured heat of adsorption (standard molar enthalpies of adsorption at 300 K) for Pb deposition onto an electron-irradiated, spin-coated PMMA at 300 K as a function of metal coverage. Each data point is due to a pulse of approximately 0.018 ML of Pb. This is an average of three experimental runs. The electron exposure was $6 \mu\text{A}/\text{cm}^2$ ($4.7 \times 10^{16} \text{ e}^-/\text{cm}^2$) of 155 eV electrons for 10 min.

increases steeply and smoothly with coverage, such that by ~ 2 ML it reaches a maximum of 200 kJ/mol. Thereafter it decreases to reach a nearly constant value of 194 kJ/mol by 8 ML, within 0.5% of the bulk heat of sublimation of Pb (195.2 kJ/mol [37]), as expected for Pb adsorbing on a Pb surface. This is within the estimated accuracy of the absolute calibration of this calorimeter ($\sim 2\%$). The standard deviation about a straight-line fit to the high coverage data (4–8 ML) is ± 0.7 kJ/mol, which gives a good estimate of the pulse-to-pulse standard deviation of the three-run average measurement. The standard deviation about a straight-line fit to the high coverage data for a representative individual run is ± 1.2 kJ/mol.

4. Discussion

These are the first calorimetric measurements of the adsorption energies of metal atoms on polymers where the sticking probabilities were also measured. The pulse-to-pulse standard deviations obtained here (~ 1 kJ/mol) are at least as good as those observed in the only other calorimetric measurements of metal adsorption energies on polymers [23,24], where the sticking probability was assumed to be unity. The absolute accuracy is markedly improved in the current design, since those earlier measurements were calibrated by assuming the heat at high coverage equals the bulk heat of sublimation, and since they also assumed unit sticking probability [23,24].

4.1. Pb on pristine PMMA

The measured heats, as presented in Fig. 4, are comprised of two contributions: (1) the thermal energy which the hot metal gas atoms impart to the substrate when they encounter its surface, and (2) the energy associated with bond formation at the surface, both metal/polymer and metal/metal. The degree to which hot gas atoms transfer their thermal energy to colder surfaces upon collision is quantified by their thermal accommodation coefficient (α), defined as [38]

$$\alpha = (KE_{\text{init}} - KE_{\text{after}})/(KE_{\text{init}} - 2RT_{\text{sample}}),$$

where KE_{init} is the average initial kinetic energy of the gas, KE_{after} is the average final kinetic energy of the gas after collision with the surface, and $2RT_{\text{sample}}$ is the final average kinetic energy they would have if they left the surface in a Maxwell–Boltzmann distribution at the sample temperature (T_{sample}), as would be the case for equilibrium with both gas and solid at T_{sample} [39]. Metal atoms which trap long enough for energy equilibration before reentering the gas phase will completely thermally accommodate ($\alpha = 1$), while metal atoms which are only briefly trapped and rapidly reenter the gas phase may only partially accommodate ($\alpha < 1$). As described in [26], the average kinetic energy of metal atoms heated in a Knudsen cell and collimated by a series of apertures is well-defined and can be calculated from the oven temperature ($2RT_{\text{oven}}$ where $T_{\text{oven}} = 1120$ K). Thus, the maximum thermal energy that Pb gas atoms can release into the substrate before reentering the gas phase is given by $(KE_{\text{init}} - KE_{\text{after}}) = \alpha(2RT_{\text{oven}} - 2RT_{\text{sample}})$, with $\alpha = 1.0$. (Here, $T_{\text{sample}} = 300$ K.). This gives a maximum energy transfer to the sample of 13.6 kJ/mol_{dosed}. This is approximately 1 kJ/mol_{dosed} larger than the measured heats shown in Fig. 4, indicating that the non-sticking metal atoms must come off the surface hotter than 300 K. How much hotter depends sensitively on the exact value of the sticking probability and heat of adsorption here, neither of which is well known. In any case, this incomplete thermal accommodation (<93%) highlights the extremely weak attraction between Pb and pristine PMMA.

Accurately estimating the accommodation factor is difficult in this case, as a portion of the energy measured inevitably arises from limited bond formation from the small fraction of metal atoms which do actually stick irreversibly, which could conceivably produce heats per metal atom that are an order of magnitude larger than that generated by thermal accommodation. Small absolute errors in the measured sticking probability (associated with small absolute errors in measuring the zero-sticking reference signal by the mass spectrometer) lead to large relative errors in the measurement of a small sticking probability, as in this case. This generates large errors in assigning the proper fractions of the measured heats due to

thermal accommodation compared to surface bond formation. Doubling the sticking probability (which is just within the possible error range associated with the sticking measurement shown in Fig. 2) would double the contribution of the much larger energy bond formation component, resulting in a marked reduction in the energy arising from thermal accommodation of the non-sticking fraction. This would mean that the metal atoms that do not stick have a very low accommodation coefficient, suggesting an even weaker Pb–PMMA interaction.

Given the weak interaction involved, if there is any permanent bond formation occurring on the pristine surface it is most likely due to Pb adatoms trapping at Pb clusters on the surface. Similar behavior is seen in Cu deposition on PMDA–ODA, where the heats measured were proposed to be dominated by Cu–Cu interactions [23]. Converting the energies shown in Fig. 4 into an “energy per mol adsorbed” basis requires multiplying the mol_{dosed} by the sticking probability found at that dosed coverage. As mentioned previously, given the small sticking probability shown in Fig. 2, small absolute errors in the sticking probability can lead to a large degree of error in assigning the heats in a per mol adsorbed basis. This error is magnified by our lack of knowledge of how much heat to assign to thermal accommodation of the non-sticking fraction, so that reporting heats on this basis is unreasonable and not done here.

Given that the sticking probability shown in Fig. 2 does not appreciably increase over the entire range of amount up to 10 ML dosed, and the observed short residence time of any transient adsorbates on the surface, it seems unlikely that critical nuclei form at all or only do so at very low concentrations on (or in) the PMMA [40]. If there were critical nuclei at the surface (or subsurface) region probed by Pb atoms, they would eventually grow in size and increase the sticking probability [35]. Critical nuclei are usually assumed to be dimers during metal film growth, but can be larger [41].

The inertness of the pristine PMMA surface, showing a very low sticking probability and small heats of adsorption is somewhat surprising given

the presence of an ester functional group which is thought to be reactive [11,18]. However, more reactive vapor deposited metals such as Cu and Ni also have shown poor to moderate interaction with the pristine PMMA surface, nucleating into particles [9]. The only vapor deposited metal that has been studied to our knowledge which seems to react strongly with PMMA, forming a wetting layer on the surface, is Al [9]. (One also would expect more aggressive metals like Cr and Ti to exhibit similar behavior to Al on this particular substrate, since they do on PMDA–ODA [42, 43].) The PMMA surface may be more inert than expected if its ester group points inward towards the bulk, as has been suggested [18].

Low sticking probabilities for weakly reacting metals have been seen on other polymers at room temperature. Faupel et al. measured a number of “condensation coefficients”, or sticking probabilities, for noble metal adsorption onto a variety of polymers by XPS and radiotracer methods [44]. On Teflon, Ag, Au and Cu have initial sticking probabilities of 0.002, 0.006 and 0.02, respectively. Polystyrene, which has a glass transition temperature similar to PMMA, shows sticking probabilities of 0.11, 0.24, and 0.26 for Ag, Au and Cu, respectively. TMC-polycarbonate, which has an oxygen functionality like PMMA, exhibits sticking probabilities of 0.12, 0.27 and 0.73 for Ag, Au and Cu, respectively. These series of sticking probabilities seem to mirror those seen for metal adsorption onto oxide surfaces, where the order of increasing sticking probabilities runs as $\text{Pb} < \text{Ag} < \text{Cu}$ [45], suggesting that Pb would exhibit a sticking probability smaller than ~ 0.12 on polymers like TMC-polycarbonate, polystyrene and PMMA, as observed here. Although low sticking probabilities for these metals on polymers seem to be the norm, Ag, Au and Cu all have large initial sticking probabilities of 0.95 on PMDA–ODA [44].

4.2. Pb on electron-irradiated PMMA

Exposing the PMMA surface to an electron beam greatly increases its reactivity. The initial sticking probability is dramatically larger compared to the undamaged polymer surface (see Fig. 3), and the initial heat of adsorption increases

from $<13 \text{ kJ/mol}_{\text{dosed}}$ to $134 \text{ kJ/mol}_{\text{adsorbed}}$ (see Fig. 5). This proves that the electron exposure creates some variety of defects on the surface that bind Pb adatoms more strongly. Further, whereas the sticking probability on the pristine surface remains constant, the electron irradiated PMMA surface shows a sticking probability that increases with increasing coverage (Fig. 3).

This increase in sticking probability with dosed amount is very similar to other non-unit sticking systems such as Pb adsorption on Mo oxide, MgO and hydroxylated-MgO where the Pb adatoms readily diffuse across the surface and nucleate Pb clusters at defect sites or find an existing Pb clusters upon which to attach [34–36]. As the coverage increases, so does the sticking probability, indicating that the size of the Pb islands decorating the surface are increasing in area to the point where the distances between them is within the mean free path of a diffusing Pb adatom while transiently trapped on the PMMA surface.

The coverage dependence of the heats of adsorption shown in Fig. 4 also is reminiscent of Pb and late transition metal adsorption on oxide surfaces [34–36,45]. A low initial heat of adsorption indicates weak interaction between the adatom and the surface. As with metals on oxides [34–36], we will attribute this coverage dependence mainly to the growth of 3D particles of metal as the coverage increases. The initial heat of adsorption is much higher than on the pristine PMMA surface, showing that the binding of Pb is stronger at defects. However, the initial heat of adsorption probably cannot be attributed to an adsorption event at any single type of polymer defect, but an average of all the available defect environments, with possible additional contributions to the fact that Pb–Pb bonds are also being formed as Pb clusters nucleate and grow even possibly during the duration of the first 0.018 ML metal pulse.

As the metal coverage increases, the Pb particle size increases, driving the heats closer to the heat of sublimation as the likelihood of finding a bulk-like adsorption site (i.e., one with 6 Pb nearest neighbors) for deposited Pb adatoms increases. The closeness of the final adsorption energy to the bulk Pb sublimation energy also points to a model where the adsorbed Pb stays at the surface to

create a pure metal thin film rather than diffusing into the bulk of the polymer.

The lower initial heat of adsorption relative to that at high coverage is therefore attributed to a combination of two effects: (1) the bonding of the metal to the polymer is much weaker even at electron-induced defects sites than the bonding of metal atoms when they adsorb on a bulk Pb surface, and (2) the metal clusters are still very small in the first metal pulse, so that the Pb atoms which add to these clusters make fewer Pb–Pb nearest neighbor bonds than they do when they adsorb on the surface of bulk Pb. Adsorption onto bulk Pb is the reverse of sublimation, and can be thought of mechanistically as adsorption at a kink site on a stepped Pb(1 1 1) surface, where it forms six Pb–Pb nearest-neighbor bonds. As with metal adsorption on oxides [34–36], we assume that as the Pb coverage increases, the Pb particle size grows and so the Pb atoms which add to these clusters make more and more Pb–Pb nearest neighbors bonds. Eventually the large Pb islands coalesce, and at high coverages the deposited Pb adsorbs onto bulk-like Pb sites.

5. Conclusion

The sticking probability and heats of adsorption for Pb deposited on spin-coated “pristine” PMMA surfaces and electron irradiated PMMA surfaces at 300 K have been measured. This is the first experiment to show the feasibility of spin coating a polymer directly onto a PVDF pyroelectric polymer detector to measure heats of adsorption. The resulting precision (~ 1 kJ/mol pulse-to-pulse standard deviation) and absolute accuracy ($\sim 2\%$) are much better than any prior calorimetric measurements of adsorption energies on polymer surfaces. This is the first measurement of adsorption energies of any metal onto any polymer surface where the results were supported with in situ sticking probability measurements. The sticking and calorimetry for Pb deposition on the pristine PMMA surface indicates that the metal gas does not react with the substrate at all, but imparts only a fraction of its thermal energy to the substrate when it scatters from the polymer surface. Deposi-

tion of Pb on electron-irradiated PMMA exhibited a stronger, although still relatively weak, Pb adatom/polymer substrate interaction. Electron bombardment creates bond scission in the polymer chains and forms nucleation centers for Pb island formation, much the same way as oxygen vacancies nucleate metal clusters on oxides. This is manifested in an increase by more than an order of magnitude in the initial sticking probability, and an increase in the initial heat of adsorption from <14 kJ/mol_{dosed} to 134 kJ/mol_{adsorbed}. Eventually the Pb islands grow in size, and at high coverages the deposited Pb adsorbs onto bulk-like Pb sites.

Acknowledgements

The authors would like to acknowledge the National Science Foundation, for support of this work. We would also like to thank Winston Ciri-don and Libby R. Heeb for their assistance in spin coating the samples, and J. Todd Stuckless for very helpful advice and information.

Appendix A

The calorimeter’s sample/heat detector (i.e., the PVDF sheet spin-coated on one face with PMMA) was clamped onto a specially designed sample/calorimeter platen shown in Fig. A1 by a Cu face plate, which retains the PVDF sheet, but which has a 8 mm diameter hole to expose part of the polymer-coated PVDF sheet for adsorption. This Cu plate electrically connects the front PVDF face to the main body of the platen, which is held at electrical ground (chamber ground). The back face of the PVDF is in contact with a bolt which sticks out of the back of the platen, as shown, to provide the signal voltage. When mounted in the platen holder for calorimetry, this bolt is connected via a shielded electrical vacuum feedthru and shielded cable to the input of a preamplifier described elsewhere [26].

The outer body of the sample platen is a disc with two parallel grooves around its perimeter which are used for picking it up with (and transferring it between) fork-like platen transfer grips,

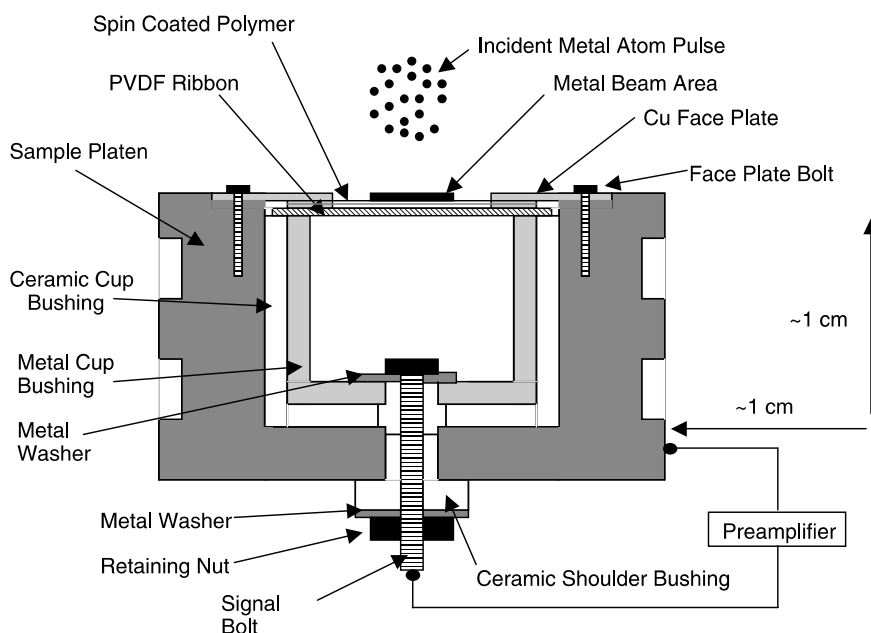


Fig. A1. Adsorption calorimeter for spin-coated polymer samples mounted in a transferable platen. This entire sample/calorimeter platen (except the face-plate bolts) is circularly symmetric when viewed from above or below. A circular cut-out of a metallized PVDF sheet is spin-coated with the polymer of choice onto its front face, and it is clamped between a copper face plate and copper cup bushing (dark gray). A 4-mm diameter area centered on its front face is irradiated by metal pulses from the metal atom beam. The copper cup bushing is held in the ceramic cup bushing by a signal bolt which is isolated from the sample holder (light gray). The front and back face of the PVDF are thus electrically isolated from each other, and the signal bolt and sample holder act as the electrical leads to the preamplifier.

following a design very similar to that of a commercial sample transfer system (the Thermionics SPF Series Dual Groove Disc System which includes the SPFP sample platen, the SPFF sample fork/transfer grip and the SPFD platen dock).

The spin-coated polymer samples are single-use substrates; once they are dosed with metal, they are discarded and a new sample is introduced to the UHV chamber. A sample platen carriage capable of holding up to 8 sample platens of the type shown in Fig. A1 was housed in a small, adjacent UHV chamber complete with a sample transfer system. The sample chamber is pumped by a 70 L/s Pfeiffer turbo pump backed by a mechanical pump. The chamber has an operating pressure of $\sim 8 \times 10^{-9}$ Torr after loading 8 polymer samples, without baking.

The sample platen carriage is mounted on a push-pull/rotation differentially-pumped sliding rod. The rod is sealed with two spring-energized

seals housed in a UHV feedthrough that is differentially pumped by a mechanical pump. Fig. A2 shows mechanical drawings of the sample carriage. There are two tiers, capable of holding four sample platens each. Two aluminum plates, thermally isolated by the ceramic shoulders, hold the tiers in place on the central shaft and support the block where the four sample platen forks are mounted. The upper tier is held in position with the use of two set screws in the aluminum plate while the lower tier is supported by an aluminum plate screwed into the bottom of the central shaft. The central shaft of the sample carriage is wired to a power supply and is in electrical connection with Ta foil heaters set in each tier such that the samples can be heated in vacuum to aid in the removal of residual solvent and establish polymer surface cleanliness while preserving the stability of the spin coated polymer. Thermocouples are attached to the forks to monitor sample temperature.

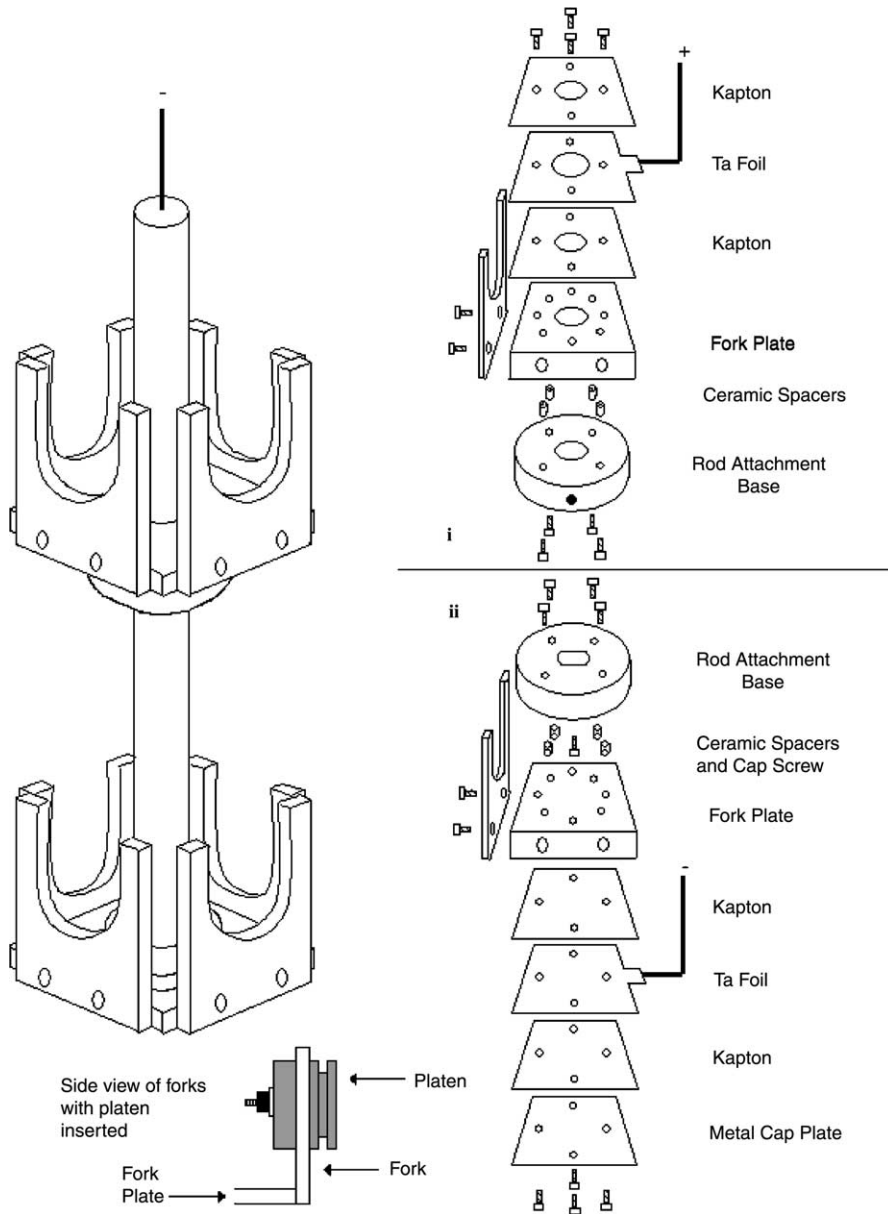


Fig. A2. Diagram of the sample platen carriage, which resides in the sample chamber adjacent to the analysis/calorimeter chamber. At the bottom left is a side view of one of the forks holding a sample/calorimeter platen of the type in Fig. A1. (not to scale). (i) Components of the upper tier, which is held to the central shaft by a set screw in the rod attachment base and thermally isolated from the sample forks by ceramic spacers. The Ta foils are used as resistive heaters to heat the fork plates. They are wired in parallel, both being electrically connected to the central shaft. (ii) Components of the lower tier, which is held to the central shaft by a cap screw from the bottom of the rod attachment base and thermally isolated from the sample forks by ceramic spacers. Electrical connections are highlighted in black.

Sample platens are shuttled from the sample chamber to the analysis/calorimeter chamber with

the use of a sample transfer rod which is mounted perpendicular to the sample platen carriage's shaft

and can be translated and rotated. Like the central shaft of the sample carriage, the transfer rod is also sealed with spring energized seals and differentially pumped by mechanical pumps. Sample platens can be placed onto a fork located on the end of the transfer rod from the sample carriage and shuttled into the UHV analysis chamber (through the gate valve which isolates it from the sample chamber), to be picked up by a fork on the $XYZ\theta$ manipulator. A sample on the analysis chamber's manipulator also may be transferred back to the sample carriage.

References

- [1] W. Goldie, *Metallic Coating of Plastics*, Electrochemical Publications Limited, Middlesex, England, 1968.
- [2] T.J. Marks, J.G.C. Veinot, J. Cui, H. Yan, A. Wang, N.L. Edleman, J. Ni, Q. Huang, P. Lee, N.R. Armstrong, *Synth. Metals* 127 (2002) 29.
- [3] M. Fahlman, W.R. Salaneck, *Surf. Sci.* 500 (2002) 904.
- [4] J.C. Scott, *J. Vac. Sci. Technol. A* 21 (2003) 521.
- [5] J. Pireaux, *J. Synth. Metals* 67 (1994) 39.
- [6] F. Faupel, R. Willecke, A. Thran, *Mater. Sci. Eng. R22* (1998) 1.
- [7] P.S. Ho, R. Haight, C. White, B.D. Silverman, F. Faupel, L.H. Lee (Eds.), *Fundamentals of Adhesion*, Plenum Press, New York, 1991.
- [8] V. Zaporotchenko, T. Strunskus, K. Behnke, C. Von Bechtolsheim, M. Kiene, F. Faupel, *J. Adhesion Sci. Technol.* 14 (2000) 467.
- [9] P. Bebin, R.E. Prud'homme, *Chem. Mater.* 15 (2003) 965.
- [10] A.J. Wagner, G.M. Wolfe, D.H. Fairbrother, *Appl. Surf. Sci.* 219 (2003) 317.
- [11] A.K. Oultache, R.E. Prud'homme, *Polym. Adv. Technol.* 11 (2000) 316.
- [12] C.-M. Chan, *Polymer Surface Modification and Characterization*, Hanser Publishers, Munich Vienna, NY, 1994.
- [13] G. Jorgensen, P. Schissel, in: K.L. Mittal, J.R. Susko (Eds.), *Metallized Plastics I: Fundamental and Applied Aspects*, Plenum Press, New York, 1989.
- [14] P. Schissel, C. Kennedy, R. Goggin, *J. Adhesion Sci. Technol.* 9 (1995) 413.
- [15] I. Adesida, C. Anderson, E.D. Wolf, *J. Vac. Sci. Technol. B* 1 (1983) 1182.
- [16] P. Bebin, R.E. Prud'homme, *J. Polym. Sci. Pol. Phys.* 40 (2002) 82.
- [17] R.L.W. Smithson, D.J. McClure, D.F. Evans, *Thin Solid Films* 307 (1997) 110.
- [18] P. Bertrand, P. Lambert, Y. Travaly, *Nucl. Instr. Mech. Phys. Res. B* 131 (1997) 71.
- [19] S. Pignataro, *Surf. Interf. Anal.* 19 (1992) 275.
- [20] V.M. Bermudez, *J. Vac. Sci. Technol. B* 17 (1999) 2512.
- [21] J. Zekonyte, J. Erichsen, V. Zaporotchenko, F. Faupel, *Surf. Sci.* 532–535 (2003) 1040.
- [22] R. Murdey, J.S. Liang, J.T. Stuckless, *Rev. Sci. Instrum.* 76 (2005) 023911.
- [23] R. Murdey, J.T. Stuckless, *J. Am. Chem. Soc.* 125 (2003) 3995.
- [24] S.S. Hon, J. Richter, J.T. Stuckless, *Chem. Phys. Lett.* 385 (2004) 92.
- [25] C.E. Borroni-Bird, D.A. King, *Rev. Sci. Instrum.* 62 (1991) 2177.
- [26] J.T. Stuckless, N.A. Frei, C.T. Campbell, *Rev. Sci. Instrum.* 69 (1998) 2427.
- [27] H. Ihm, H.M. Ajo, J.M. Gottfried, P. Bera, C.T. Campbell, *J. Phys. Chem. B* 108 (2004) 14627.
- [28] S.F. Diaz, J.F. Zhu, N. Shamir, C.T. Campbell, *Sensors Actuators B* 107 (2005) 454.
- [29] D.E. Starr, C.T. Campbell, *J. Phys. Chem. B* 105 (2001) 3776.
- [30] C.B. Walsh, E.I. Frances, *Thin Solid Films* 347 (1999) 167.
- [31] D.A. King, M.G. Wells, *Surf. Sci.* 29 (1972) 454.
- [32] S.W. Pauls, C.T. Campbell, *Surf. Sci.* 226 (1990) 250.
- [33] D.E. Starr, Microcalorimetric heats of adsorption, surface residence times and sticking probabilities of metals on metal-oxide, and silicon substrates, University of Washington, Seattle, 2001.
- [34] J.T. Stuckless, D.E. Starr, D.J. Bald, C.T. Campbell, *J. Chem. Phys.* 107 (1997) 5547.
- [35] D.E. Starr, D.J. Bald, J.E. Musgrove, J.T. Ranney, C.T. Campbell, *J. Chem. Phys.* 114 (2001) 3752.
- [36] D.E. Starr, S.F. Diaz, J.E. Musgrove, J.T. Ranney, D.J. Bald, L. Nelen, H. Ihm, C.T. Campbell, *Surf. Sci.* 515 (2002) 13.
- [37] D.R. Lide (Ed.), *CRC Handbook of Chemistry and Physics*, CRC Press, Boca Raton, 1990.
- [38] D. Auerbach, C. Becker, J. Cowin, L. Wharton, *Appl. Phys.* 14 (1977) 141.
- [39] G. Comsa, R. David, *Surf. Sci. Rep.* 5 (1985) 145.
- [40] V. Zaporotchenko, T. Strunskus, K. Behnke, C. Von Bechtolsheim, M. Kiene, F. Faupel, *J. Adhesion Sci. Technol.* 14 (2000) 467.
- [41] C.T. Campbell, *Surf. Sci. Rep.* 27 (1997) 1.
- [42] P.S. Ho, R. Haight, R.C. White, B.D. Silverman, L.H. Lee (Eds.), *Fundamentals of Adhesion*, Plenum, New York, 1991.
- [43] F.S. Ohuchi, S.C. Freilich, *J. Vac. Sci. Technol. A6* (1988) 1004.
- [44] V. Zaporotchenko, K. Behnke, A. Thran, T. Strunskus, F. Faupel, *Appl. Surf. Sci.* 144–145 (1999) 355.
- [45] C.T. Campbell, D.E. Starr, *J. Am. Chem. Soc.* 124 (2002) 9212.